Investigation of excitonic saturation by time-resolved circular dichroism in GaAs-AlxGa1-xAs multiple quantum wells

Investigation of excitonic saturation by time-resolved circular dichroism in GaAs-$Al_xGa_{1-x}As$ multiple quantum wells

M. J. Snelling* and P. Perozzo
Center for Research in Electro-Optics and Lasers, University of Central Florida, Orlando, Florida 32826

D. C. Hutchings
Department of Electronics and Electrical Engineering, University of Glasgow, Glasgow G12 8QQ, United Kingdom

I. Galbraith
Department of Physics, Heriot-Watt University, Edinburgh EH14 4AS, United Kingdom

A. Miller†
Department of Physics and Astronomy, University of St. Andrews, St. Andrews, Fife KY19 9SS, United Kingdom
(Received 8 February 1994)

Time- and wavelength-resolved circular dichroism of the excitonic saturation in GaAs-$Al_xGa_{1-x}As$ multiple quantum wells at room temperature is investigated using a degenerate excite-probe method. For moderate excitation, the effects of photogenerated carriers on the heavy-hole exciton resonance are separately identified as the contributions of phase-space filling and Coulombic effects (screening and line-shape broadening). These contributions are observed to be of a similar magnitude. The induced circular dichroism of the exciton saturation was observed to decay with a time constant of 50 ps, which is attributable to electron spin relaxation.

I. INTRODUCTION

Quantum-well devices are finding applications as photodetectors, optical modulators, and all-optical switching elements.[1] However, one of the fundamental limitations to the performance of these devices at high optical power levels is the role of exciton saturation (the change in the optical spectrum due to the presence of a high density of photogenerated carriers).

There are essentially two mechanisms which contribute to exciton saturation; Pauli exclusion effects such as phase-space filling and Coulombic effects such as screening and the related exciton line-shape broadening. Schmitt-Rink *et al.*[2] considered the small signal reduction in the exciton oscillator strength due to phase-space filling and Coulombic effects (not including broadening) induced by an electron-hole plasma. In that paper, the Coulombic effect on the oscillator strength was split into two contributions; a long-range, classical screening term (independent of the energy distribution of the plasma) and a short-range term which was denoted as an exchange contribution (dependent on the plasma energy distribution). It was subsequently shown that the classical screening term is negligible in quantum-well systems. This was verified experimentally using a nonthermal electron-hole plasma generated by exciting at a frequency well above the band edge (with $\simeq$ 100 fs resolution).[3] However, it was also shown that the remaining Coulombic contribution (exchange) and the phase-space filling contribution give rise to optical effects of a similar magnitude. Unfortunately, this separation of Coulombic terms (where one was shown to be negligible) has led to the popular misconception that all Coulombic effects are negligible compared to Pauli exclusion effects in two-dimensional systems.

In order to investigate the different contributions from Coulombic and Pauli exclusion effects it is necessary to employ nonequilibrium carrier distributions. Exciting into the continuum states[3] allows the long-range screening effects to be separated; however, the other contributions cannot be easily distinguished. An alternative method of generating a nonequilibrium carrier distribution is to use a circularly polarized pump to selectively populate only one spin orientation. The heavy-hole/conduction band transition in zinc-blende semiconductors has selection rules which dictate that only one spin orientation of the electrons and heavy holes is excited for a given orientation of circularly polarized light (Fig. 1). The light-hole states consist of mixed spins and do not have this restriction, and hence in bulk semiconductors it is difficult to achieve complete spin selectivity. However, in quantum wells the heavy-hole/light-hole degeneracy is lifted and complete optical spin selectivity is possible.

Previous room temperature investigations of exciton saturation employed linearly polarized light and hence the Pauli exclusion and Coulombic effects could not be individually resolved.[3,4] There have been a number of recent studies at low temperatures using circular polarizations. In particular, time-resolved excite-probe dichroism measurements where a comparison was performed between when excite and probe pulses were circularly polarized in the same and opposite senses have been employed.[5,6] Stark *et al.*[5] observed such a dichroism at a temperature of 4 K, but as the excite wavelength was above the light-hole exciton resonance, both spin states

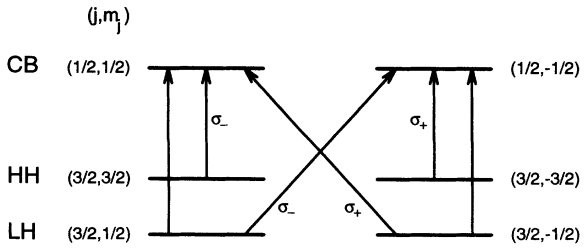

FIG. 1. Schematic showing the selection rules for the transitions from the heavy-hole and light-hole valence bands to conduction band. The (j, m_j) refer to the quantum numbers for angular momentum and its component along one direction. The σ_+ and σ_- refer to the transitions excited by each sense of circularly polarized light and correspond to $\Delta m_j = \pm 1$, respectively, where the propagation direction is used to define m_j.

are excited (though unequally) and hence it is difficult to make a quantitative statement. Bar-Ad and Bar-Joseph[6] used a wavelength such that only the heavy-hole exciton is excited and hence obtained absolute spin selectivity. In addition the longer delay times allowed the estimation of both hole and electron spin relaxation times. However, at low temperatures the carrier statistics are quite different compared to room temperature. First, at low temperatures, the excitons will remain un-ionized and hence it will be exciton-exciton effects which dominate rather than the plasma-induced exciton saturation applicable at room temperature. For example, Bar-Ad and Bar-Joseph[6] obtain quantum beats between the exciton and biexciton resonances when excite and probe pulses were oppositely circularly polarized at temperatures of up to 60 K. Second, even if an electron-hole plasma could be sustained, the carrier statistics would have a high degree of degeneracy. As will be shown later in this paper, in the Boltzmann limit (moderate excitation at room temperature) the circular dichroism can be identified solely with Pauli exclusion effects.

A number of different mechanisms have been proposed to account for spin relaxation in semiconductors. The two mechanisms believed to be dominant in quantum wells[7] are as follows. (i) The mechanism proposed by D'Yakonov and Perel'[8] based on the fact that the degeneracy of the conduction band is lifted for crystals that lack inversion symmetry, which is the case in III-V semiconductors. The spin splitting of the conduction band can be considered as the source of a pseudomagnetic field. This pertubating field causes the electron spins to precess, thereby providing a mechanism for relaxation. This mechanism dominates at low acceptor concentration and high temperatures.[9] (ii) The mechanism proposed by Bir, Aronov, and Pikus[10] based on an exchange interaction between an electron and hole. In this process the electron and hole exchange spins through a magnetic interaction. This is believed to be the dominant mechanism for high hole densities (e.g., heavily p-doped material or high optical excitation) and low temperatures.[11,12]

In this paper we consider the temporal and wavelength dependence of the circular dichroism of the exciton saturation at room temperature. Experimentally this is performed by using an excite-probe configuration with various polarization configurations, which allows the alteration of the occupation of phase-space while keeping a constant carrier concentration. Two theoretical approaches will be taken to analyze the exciton saturation dichroism. First, a full numerical solution of the Wannier equation will be performed using the single plasmon pole approximation for the screened Coulomb potential. The effects of density-dependent broadening will also be included in this approach and are essential to correctly predict the wavelength dependence of the exciton saturation. Second, an approximate analytical solution will be obtained for the change in oscillator strength using a simpler Debye screened potential. In this paper we will use the term screening to apply to all processes which reduce the Coulombic interaction, whether they be classical or quantum mechanical in nature.

II. EXPERIMENTAL

A. Description

The experimental system consisted of a cavity-dumped, mode-locked Styryl 9 dye laser producing pulses with a full width at half maximum of less than 1 ps at a repetition rate of 7.6 MHz. The beam was split to form excite and probe pulses, and by subsequent adjustment of the probe path length, the time of arrival of the probe pulses at the sample could be varied with respect to that of the excite pulses. The excite and probe beams were separately attenuated to average powers of 200 μW and 20 μW, respectively, and the excite beam was chopped for subsequent phase-sensitive detection. These optical power levels were low enough to ensure that the measured transmission change was directly proportional to the excite power, while still having an adequate signal to noise ratio. Each of these beams was passed through a suitably oriented linear polarizer followed by a quarter wave plate to produce either left or right handed circularly polarized light, or linearly polarized light. Three separate excite and probe polarization configurations were used in the following measurements: pump and probe of orthogonal linear polarization (OLP), excite and probe circularly polarized in the same sense (SCP), and excite and probe circularly polarized in opposite senses (OCP).

The sample consisted of 120 periods of 6.5 nm GaAs quantum wells surrounded by 21.2 nm $Al_{0.4}Ga_{0.6}As$ barriers. The background doping was 10^{16} cm^{-3} p type. The GaAs substrate was etched off, to allow measurements to be made in transmission, and an anti-reflection coating applied to both of the sample's surfaces. Finally, the structure was bonded on a sapphire base for the purpose of mechanical stability and heat sinking. The carrier recombination time for this sample has been determined to be 70 ns.[4] Figure 2(a) shows the linear (low-power) transmission of the multiple-quantum-well (MQW) sample. Both the heavy-hole and light-hole exciton resonances are clearly resolved at 830 and 821 nm, respectively.

In all the following excite-probe measurements, regardless of polarization, there is an observed increase in trans-

mission at negative delays (when the probe pulse precedes the excite pulse). This background signal was observed to be independent of the polarization of either the excite or probe pulses. Additionally, at long wavelengths, where there should be a negligible carrier density excited, an increase in transmission is also observed. In the case of the probe preceding the excite pulse, the previous excite pulse precedes the probe by 130 ns; hence the background signal is unlikely to be due to carrier effects. In addition, decreasing the pulse repetition rate, while increasing the laser power such that the energy per pulse incident on the sample remained constant (i.e., keeping the photoexcited carrier density constant but decreasing the average incident power) reduced these background effects leaving the faster signals unaltered. It is assumed that the background signal is due to a combination of sample heating and scattering of the excite pulse. Hence, since it is the carrier-induced effects which are of interest here, this background signal (obtained at negative delays) will be subtracted from all the results.

B. Results

In order to investigate the wavelength dependence of the exciton saturation dichroism, the probe pulses were set to arrive just after (4 ps) those from the excite beam, and the excitation wavelength was scanned across the heavy-hole exciton resonance. This was performed for each of three beam polarization configurations considered. The results of this are shown plotted in Fig. 2(b) where the change in absorption is calculated from the observed change in transmission ΔT by $\Delta\alpha \propto -\Delta T/T$ where T denotes the linear transmission of the sample. It can be seen in all three polarization cases that the major feature is a decrease in absorption at the heavy-hole exciton peak with a small feature giving an increase in absorption on the long wavelength side. The increased absorption on the long wavelength side of the exciton peak can be explained by an increase in the linewidth. The wavelength dependence shown here, however, is strongly modified by the fact that this is a single-wavelength experiment and the variation in linear absorption gives a variation of excited carrier density with wavelength. In an attempt to eliminate this carrier density variation, we divide this absorption change by $(T_{\max} - T)$ where $T_{\max}$ denotes the maximum measured linear transmission (occurring at the longest wavelengths used). This should provide a rudimentary measure of the excited carrier density (since the excite power level is held approximately constant). The calculated absorption cross

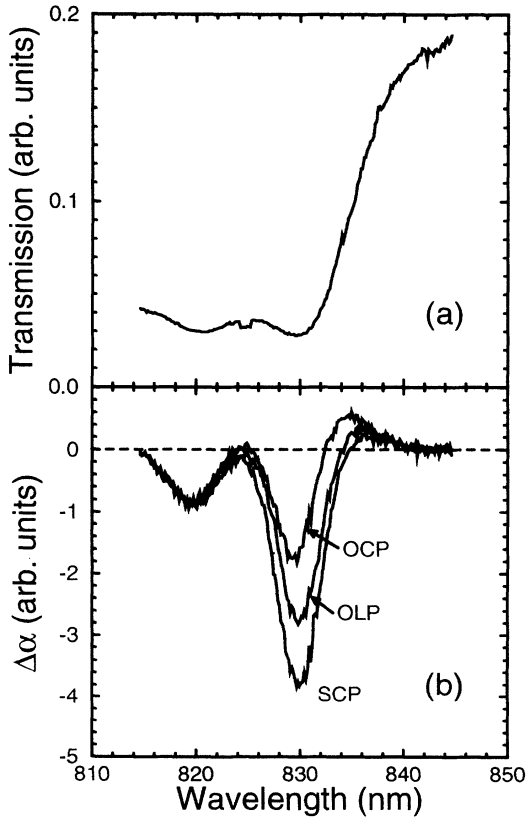

FIG. 2. (a) The wavelength dependence of the linear (low-power) transmission of the MQW sample. Both the heavy-hole and light-hole exciton resonances are resolved. (b) The wavelength dependence of the change in absorption of a probe pulse due to an excite pulse which precedes it by 4 ps, for each of the three optical polarization configurations.

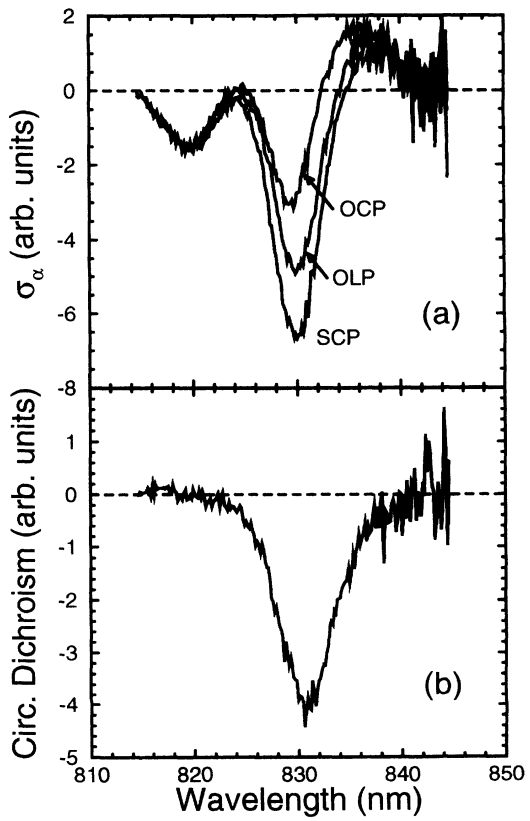

FIG. 3. (a) The absorption cross section obtained by dividing the change in absorption shown in Fig. 2(b) by $T_{\max} - T$ (which should give a measure of the excited carrier density) obtained from Fig. 2(a) for each of the three optical polarization configurations shown. (b) The circular dichroism of the absorption cross section.

section σ_α (change of absorption coefficient per unit carrier density) is shown in Fig. 3(a), in which the long wavelength features are enhanced. Figure 3(b) shows the circular dichroism of this calculated absorption cross section, $\sigma_\alpha(\mathrm{SCP}) - \sigma_\alpha(\mathrm{OCP})$.

In order to investigate the temporal evolution of the exciton saturation dichroism, the laser wavelength was tuned to the heavy-hole exciton resonance and the change in probe absorption was determined as a function of time delay between excite and probe pulses for the three polarization configurations. These results are shown in Fig. 4(a). The scan with the beams orthogonally linearly polarized (OLP) is seen to have an initial decrease in absorption which then remains constant over the range of time delays used in the experiment. However, when the two beams have the same circular polarization (SCP) the initial decrease in absorption is seen to be enhanced followed by a gradual absorption increase to the same value attained in the orthogonal linearly polarized case. The converse is true when the beams are oppositely polarized (OCP). Now the initial magnitude of the decrease in absorption is reduced but then recovers to the same value attained by the orthogonal linearly polarized transmission.

The laser was also detuned by 5 nm to the long wavelength side of the heavy-hole exciton resonance. The excite-probe scans as a function of delay are displayed in Fig. 4(b). The OLP absorption is observed to increase at this wavelength due to the effects of density-dependent broadening. The initial increase in absorption is larger for the OCP case (again attributable to density-dependent broadening) but there is almost no initial change in absorption for the SCP case. In a similar manner to the temporal scans at the peak of the heavy-hole exciton resonance, the OCP absorption decreases and the SCP absorption increases, both asymptotically approaching the OLP value (which is essentially constant on this time scale). However, these results differ from the previous set in that the long-lived component corresponds to a small absorption increase.

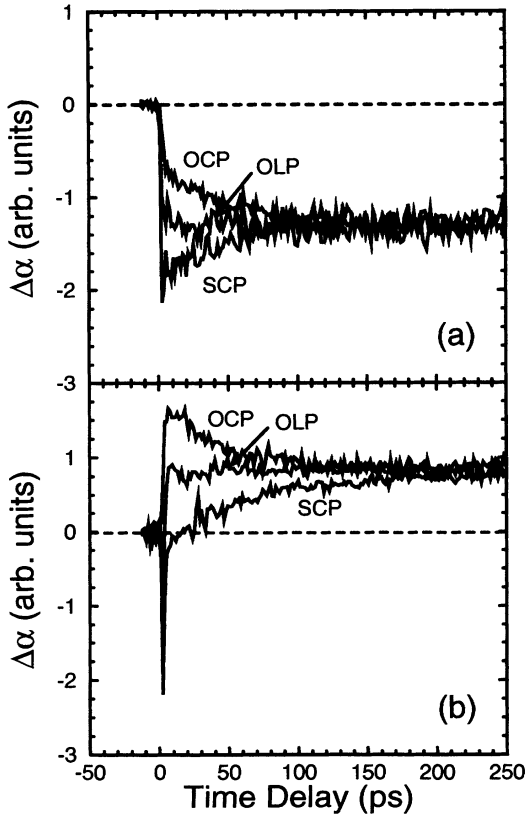

FIG. 4. The dependence of the change in probe absorption with the delay time between excite and probe pulses for each of the polarization configurations. (a) is obtained at the wavelength corresponding to the heavy-hole exciton peak. (b) is obtained at a wavelength 5 nm to the long wavelength side of the heavy-hole exciton peak.

In the case of the orthogonal linearly polarized beams the excite pulse generates equal populations of spin up and spin down electrons [Fig. 5(a)]. The probe then examines both spin states, and while there is a decrease in absorption due to the initial generation of the carriers, the recombination time is long in comparison to the range of time delays used in the experiment and no further change is observed in the transmission. However, in the case of circular polarized light, the selection rules associated with heavy-hole to conduction band transitions determine that only one spin state is excited (although the absorption coefficient has the same magnitude as in the linearly polarized case). In the situation where both pump and probe are circularly polarized in the same sense, the probe examines this same spin state [Fig. 5(b)], and initially experiences a bleached absorption. However, as the spins relax, the absorption increases, returning to the same value as that produced by the orthogonal linearly polarized beams when the spin states are equally populated.

The presence of spin-independent and spin-dependent contributions to the exciton saturation can also explain the observed behavior in the case of opposite circularly polarized beams. The probe now examines the spin state

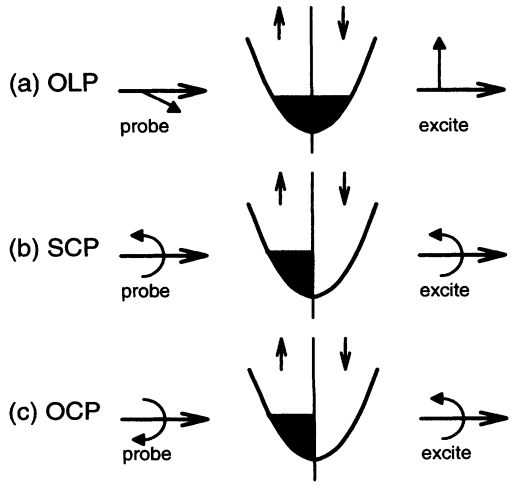

FIG. 5. Schematic showing the initial population of the two spin states for each of the three polarization configurations examined here (see text).

unpopulated by the excite pulse [Fig. 5(c)]; consequently there is a reduced initial decrease in absorption, which recovers to the value of equally populated levels as the spins relax. From our data obtained with resonant excitation of the heavy hole we obtain a spin relaxation time of 50 ps. This is slightly longer than the room temperature measurement of Takeuchi *et al.*[13], who obtained a spin relaxation time of approximately 16 ps in a superlattice consisting of thinner GaAs wells but otherwise of similar material composition. The longer spin relaxation time in wider wells repeats the trend previously observed at liquid helium temperatures.[6,14]

III. THEORETICAL

In order to understand these spin-dependent and spin-independent contributions to the absorption saturation we now consider the issue theoretically. We begin with the screened Hamiltonian for a two-band, quasi-two-dimensional semiconductor,[15]

$$\begin{aligned}\mathcal{H} = &\sum_{\mathbf{k},\sigma} E_{e,\mathbf{k}} a^{\dagger}_{\mathbf{k},\sigma} a_{\mathbf{k},\sigma} + \sum_{\mathbf{k},\sigma} E_{h,\mathbf{k}} b^{\dagger}_{-\mathbf{k},\sigma} b_{-\mathbf{k},\sigma} \\ &+\frac{1}{2} \sum_{\mathbf{k},\sigma,\mathbf{k}',\sigma'} \sum_{\mathbf{q}\neq 0} V_s(\mathbf{q}) [a^{\dagger}_{\mathbf{k}+\mathbf{q},\sigma} a^{\dagger}_{\mathbf{k}'-\mathbf{q},\sigma'} a_{\mathbf{k}',\sigma'} a_{\mathbf{k},\sigma} \\ &+b^{\dagger}_{\mathbf{k}+\mathbf{q},\sigma} b^{\dagger}_{\mathbf{k}'-\mathbf{q},\sigma'} b_{\mathbf{k}',\sigma'} b_{\mathbf{k},\sigma} \\ &-2a^{\dagger}_{\mathbf{k}+\mathbf{q},\sigma} b^{\dagger}_{\mathbf{k}'-\mathbf{q},\sigma'} b_{\mathbf{k}',\sigma'} a_{\mathbf{k},\sigma}]. \end{aligned} \tag{1}$$

The single-particle energies $E_{e,\mathbf{k}}$, $E_{h,\mathbf{k}}$ are assumed to have parabolic masses m_e and m_h. $a_{\mathbf{k},\sigma}$, $b_{\mathbf{k},\sigma}$ are the annihilation operators for electrons and holes with spin σ, respectively. $V_s(\mathbf{q})$ is the Fourier transformed, quasi-two-dimensional, screened Coulomb potential.

The interaction Hamiltonian describing the coupling of the light to the polarization is, in the dipole approximation,

$$\mathcal{H}_{\mathcal{I}} = \sum_{\mathbf{k}} [d_{\mathbf{k}} E_{\sigma_p}(t) a^{\dagger}_{\mathbf{k},\sigma_p} b^{\dagger}_{-\mathbf{k},\sigma_p} + \text{c.c.}], \tag{2}$$

where $E_{\sigma_p}(t)$ is the probe optical field and $d_{\mathbf{k}}$ is the dipole moment [proportional to the modulus of the interband momentum matrix element $|\mathbf{p}_{vc}(\mathbf{k})|$] which is assumed constant for this calculation.

A. Numerical solution of the Wannier equation

Following the steps used to calculate the semiconductor Bloch equations[16] we can calculate the generalized Wannier equation

$$\begin{aligned}&\left[\hbar\omega - E_{e,\mathbf{k}} - E_{h,\mathbf{k}} - i\gamma + \Sigma_{\mathbf{k},\sigma_p}\right] \chi_{\mathbf{k},\sigma_p} \\ &\quad = (1 - f_{e,\sigma_p,\mathbf{k}} - f_{h,\sigma_p,\mathbf{k}}) \\ &\qquad \times \left[d_{\mathbf{k}} + \sum_{\mathbf{k}'} V_s(\mathbf{k}-\mathbf{k}') \chi_{\mathbf{k}',\sigma_p}\right] \end{aligned} \tag{3}$$

for the polarizability $\chi(\hbar\omega) = \sum_{\mathbf{k}} d_{\mathbf{k}} \chi_{\mathbf{k},\sigma_p}$ whose imaginary part is proportional to the absorption coefficient. The $f_{i,\sigma,\mathbf{k}}$ ($i = \{e,h\}$) are the Fermi functions describing the distribution of electrons (holes) in their energy bands. It is assumed that the carriers thermalize much more rapidly than the spins relax, so the spin bands are essentially uncoupled and each $f_{i,\sigma,\mathbf{k}}$ has its own quasichemical potential $\mu_{i,\sigma}$. If σ_x is the spin state populated by the circularly polarized excite pulse then only $f_{i,\sigma_x,\mathbf{k}}$ are nonzero initially. The other spin states become occupied later as the spins relax. A finite homogeneous linewidth γ is introduced to account for dephasing collisions. Strictly speaking this quantity is dependent on the density in two ways. First, as the carrier density increases, scattering rates increase, giving an increase in γ. But simultaneously the carrier-carrier scattering, which is nothing but the Coulomb interaction, is screened, thereby reducing the impact of any collision. The overall effect is still an increasing γ with total carrier density[17] which we take to have a phenomenological square root dependence (in two dimensions).

The real part of the self-energy is given by

$$\Sigma_{\mathbf{k},\sigma_p} = \sum_{\mathbf{k}'} f_{e,\sigma_p,\mathbf{k}} V_s(\mathbf{k}-\mathbf{k}') + \sum_{\mathbf{k}'} V_s(\mathbf{k}') - V(\mathbf{k}'). \tag{4}$$

The first of these summations is conventionally termed screened exchange and is dominated by changes in the chemical potential (i.e., phase-space filling) at low carrier densities. The second summation is conventionally termed Coulomb hole and is given by the departure of the screened Coulomb potential from its unscreened value. Within the single plasmon pole approximation[18] $V_s(\mathbf{q})$ is given by

$$V_s(\mathbf{q}) = \frac{V(\mathbf{q})}{\epsilon(\mathbf{q})} F(\mathbf{q}), \tag{5}$$

$$\frac{1}{\epsilon(\mathbf{q})} = 1 - \frac{1}{1 + q/[\kappa F(\mathbf{q})] + \nu^2_{\mathbf{q}}/\omega^2_{\text{pl}}}, \tag{6}$$

with

$$\omega^2_{\text{pl}} = \frac{2\pi e^2}{\epsilon_0 \hbar^2} \sum_{i,\sigma} \frac{n_{i,\sigma}}{m_i} q F(\mathbf{q}), \tag{7}$$

$$\nu_{\mathbf{q}} = \frac{\hbar q^2}{2(m_e + m_h)}, \tag{8}$$

$$\kappa = \frac{2\pi^2}{\epsilon_0} \sum_{i,\sigma} \frac{dn_{i,\sigma}}{d\mu_{i,\sigma}} = \sum_{i,\sigma} \frac{m_i e^2}{\epsilon_0 \hbar^2} \left[1 - \exp\left(-\frac{2\pi\hbar^2 n_{i,\sigma}}{m_i k_b T}\right)\right]. \tag{9}$$

$n_{i,\sigma}$ is the two-dimensional density in each band $i = \{e,h\}, \sigma = \{\uparrow,\downarrow\}$ and T the plasma temperature. $V(\mathbf{q})$ is the unscreened two-dimensional Coulomb potential.

The form factor $F(\mathbf{q})$ represents the deviation of the Coulomb potential from a perfect two-dimensional potential.

$$F^{ij}(\mathbf{q}) = \int dz \int dz' |\phi_i(z)|^2 |\phi_j(z')|^2 e^{-|\mathbf{q}||z-z'|}. \tag{10}$$

The superscripts indicate that, strictly speaking, the electron-electron and electron-hole interactions are different. However, if the electron and hole remain well confined by the heterostructure it is a good approximation to take $F(\mathbf{q})$ corresponding to an infinite well of thickness L. In this case the confined electron and hole envelope functions are identical, yielding

$$F(\mathbf{q}) = \frac{8}{q^2L^2 + 4\pi^2} \times \left(\frac{3|\mathbf{q}|L}{8} + \frac{\pi^2}{|\mathbf{q}|L} - \frac{4\pi^4(1 - e^{-|\mathbf{q}|L})}{q^2L^2(q^2L^2 + 4\pi^2)} \right). \quad (11)$$

We solved Eq. (3) by discretizing the $\mathbf{k}$ points on four Gaussian quadrature intervals and solving the resulting set of (typically 110) linear equations numerically. The equilibrium densities $n_{i,\sigma}$ are an input to the calculation and define the appropriate chemical potentials.

There are three cases of interest corresponding to OLP, SCP, and OCP orientations and we consider initially only times before any spin relaxation has occurred. Room temperature, T=300 K, and a well width of 6.5 nm are used. For the densities shown the broadening (γ) doubles between zero and the maximium density.

Calculated absorption spectra for the three orientations are shown in Figs. 6(a)–6(c). In the OLP case [Fig. 6(a)], both spins are excited equally and there are significant contributions to the exciton saturation both from screening and phase-space filling. The exciton peak is bleached with no spectral shift of the peak. Induced absorption is seen below the exciton resonance as a consequence of the density-dependent broadening. In Fig. 6(b) we show the OCP case and here the behavior is quite different. There is no phase-space filling, only screening of the exciton. Hence only the Coulomb hole contributes to the self-energy ($\Sigma_{\mathbf{k},\sigma_p}$). The exciton binding energy is also reduced by the screening of the electron-hole interaction. This leads to a small redshift due to band gap renormalization and a small reduction in the oscillator strength due to the screening of the exciton. However, the effects of the density-dependent broadening dominate giving a predicted absorption decrease at the exciton peak and an absorption increase on the low energy side of the exciton. In the SCP case, Fig. 6(c), the blocking of absorption into occupied states contributes to the bleaching as in the OLP case. Both screened exchange and Coulomb hole contributions to the self-energy ($\Sigma_{\mathbf{k},\sigma_p}$) are significant and phase-space filling both limits the absorption into occupied states and modifies the exciton absorption resonance. The exciton binding energy is also modified by the screening of the electron-hole interaction, but again any spectral shift is masked by the effects of the density dependent broadening. This behavior is very similar to Fig. 6(a) but now with an increased contribution from phase-space filling. On the low frequency side of the exciton resonance for low carrier densities, Coulombic effects dominate at room temperature and the absorption increases with increasing density. However, at higher densities, phase-space filling becomes the dominant process and an absorption decrease is predicted.

In Fig. 7 we compare the three cases for the same density and plot the absorption changes in each case. A comparison with Fig. 3 shows that all the experimental features are reflected in the calculated absorption cross section.

To model the influence of the spin relaxation on the absorption we allow the density, initially in one spin state, to relax exponentially into the other until equilibrium is achieved. The absorption changes are calculated as a function of time for a particular total density in both of the OCP and the SCP cases. A total carrier density of $n_i a_0^2 = 0.2$ is chosen (where the density is scaled by the three-dimensional exciton Bohr radius $a_0 = \epsilon_0\hbar^2/e^2\mu$, ϵ_0 is the dielectric constant and μ is the reduced effective mass). Initially the population is all in one spin state and the eventual equilibrium state is half this population in both spin states. Time is given in units of the spin relaxation time.

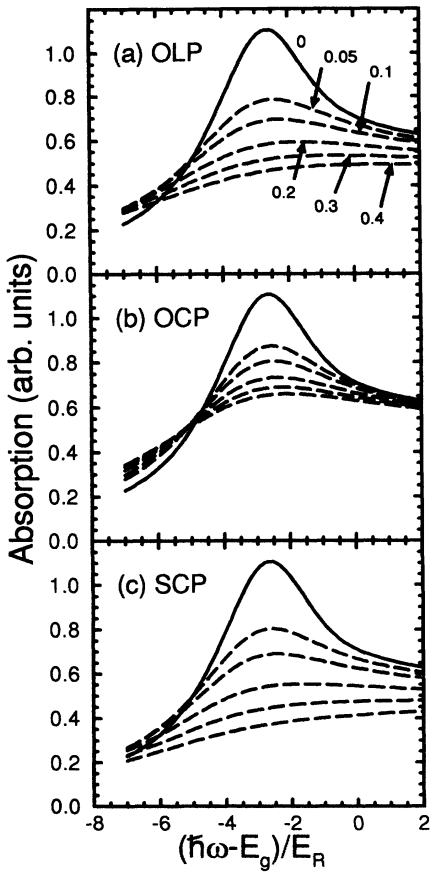

FIG. 6. The calculated excitonic absorption in the presence of an electron-hole plasma at a temperature of 300 K for (a) electron-hole population equally distributed between spin states (OLP), (b) electron-hole population entirely within the opposite spin state to that probed (OCP), and (c) electron-hole population entirely within one spin state corresponding to the probe polarization (SCP). The six curves correspond to the carrier densities na_0^2 =0 (solid), 0.05, 0.1, 0.2, 0.3, and 0.4 giving a decreasing peak absorption as indicated in (a). The frequency is normalized to the three-dimensional (3D) exciton Rydberg E_R.

The numerical results for the temporal evolution of the absorption change are shown in Fig. 8(a) at the exciton peak absorption wavelength, and in Fig. 8(b) for a wavelength on the low energy side of the exciton resonance. In both cases it is found that after the initial excitation the SCP signal increases and the OCP signal decreases, both tending to the equipopulated spin signal corresponding to the OLP case. It is also found that this OLP equilibrium signal corresponds to an absorption decrease at the peak of the exciton resonance but to an absorption increase at longer wavelengths due to increased broadening. This behavior corresponds to the experimental results in Fig. 4.

B. Analytic approximation using Debye screening

Both the theoretical and experimental results suggest that even in the absence of any phase-space filling (the OCP case) there is a substantial absorption change for GaAs quantum wells at room temperature. This contrasts strongly with the widely held notion that screening is unimportant in two-dimensional systems. In order to see this more transparently, a perturbative approach will be employed where only small signal changes to the oscillator strength for the $1s$ exciton transition are considered. This will be sufficient to describe qualitatively the density-dependent changes to the absorption at the exciton peak. For a more complete wavelength dependence of the density-dependent absorption changes, the above numerical approach must be taken.

The oscillator strength f_{1s} (essentially the area under the exciton absorption resonance) is proportional to the probability of finding both an electron and hole in the same incremental volume,[19] $f_{1s} \propto |\psi_{1s}(r=0)|^2$, where $\psi_{1s}(r)$ is the exciton (hydrogenic) wave function. In the following approach the quantum-well system will be approximated by a two-dimensional model of a semiconductor. In this limit, the binding energy of the exciton is four times its three-dimensional value $E_R^{2D} = 4E_R$. The three-dimensional binding energy can be expressed in terms of the Bohr radius as $E_R = \hbar^2/2\mu a_0^2$. However, due to the finite width and height of the wells typical exciton binding energies in quantum wells are typically only a factor of 2–3 times the three-dimensional value.

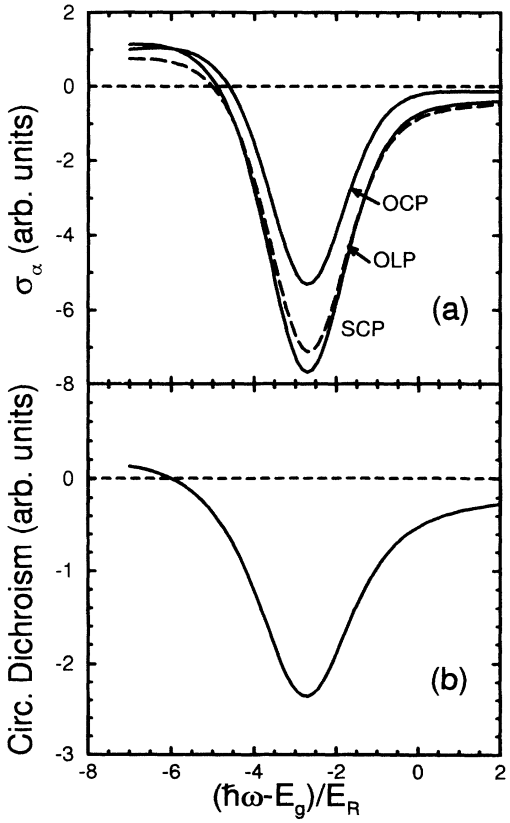

FIG. 7. (a) The calculated change in excitonic absorption from Fig. 6 for a carrier density $na_0^2 = 0.2$ for the OCP, SCP (solid lines), and OLP (dashed line) polarization cases. (b) The circular dichroism of the change in exciton absorption. These results are broadly in agreement with the equivalent experimental result shown in Fig. 3.

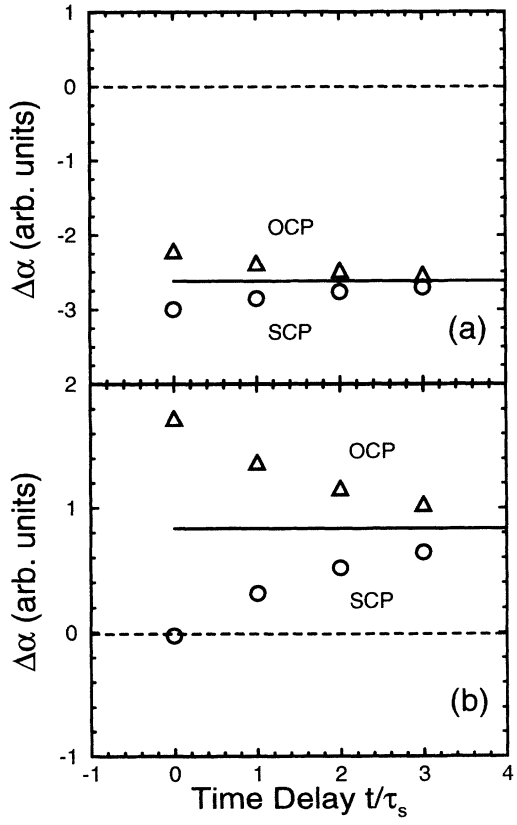

FIG. 8. The calculated absorption change as a function of time (scaled to the spin relaxation time τ_s) assuming a simple exponential spin relaxation process. The density is $na_0^2 = 0.2$. (a) corresponds to the peak exciton absorption $(\hbar\omega - E_g) = -2.7E_R$ and (b) is on the long wavelength side of the exciton resonance $(\hbar\omega - E_g) = -6E_R$. In both cases the triangles show the evolution of the OCP signal, the circles show the evolution of the SCP signal, and the solid line is the OLP signal, which is also the asymptotic limit of the other two signals.

The two-dimensional exciton wave function is given by

$$\psi_{1s}(r) = \sqrt{\frac{2}{\pi}}\frac{2}{a_0}\exp\left(-\frac{2r}{a_0}\right). \tag{12}$$

To calculate the effects of screening, the Coulomb potential in the exciton Hamiltonian will be replaced with a screened potential determined using the Debye model for a two-dimensional semiconductor. This can be obtained from the single plasmon pole screened potential given by Eq. (6) by ignoring the higher order term in q and setting the form factor to be unity, i.e., $\epsilon(\mathbf{q}) = (1+\kappa/q)$. This gives for the real space two-dimensional screened potential[20]

$$V_s(r) = -\frac{e^2}{\epsilon_0}\left[\frac{1}{r} - \kappa\int_0^\infty \frac{dq\, J_0(qr)}{q+\kappa}\right], \tag{13}$$

where J_0 is a Bessel function of the first kind and the two-dimensional screening wave number κ is given by Eq. (9). For high temperature and low carrier densities $n_i \ll m_i k_b T/\hbar^2$ (which is the situation for the experiments described in this paper) this expression can be somewhat simplified by making use of Boltzmann statistics,

$$\begin{aligned} a_0\kappa &= \pi\frac{E_R^{2D}}{k_bT}\sum_{e,h} a_0^2(n_{i,\uparrow}+n_{i,\downarrow}) \\ &= 2\pi\frac{E_R^{2D}}{k_bT}a_0^2 n_{\text{total}}^{2D}, \end{aligned} \tag{14}$$

where we use $\uparrow$ and $\downarrow$ to denote the two spin states and have scaled to the three-dimensional Bohr radius and two-dimensional exciton binding energy. Note that in the Boltzmann approximation, the screening wave number is independent of the relative populations in each spin state, only depending on the total plasma carrier density. This is not surprising since in this approximation the distribution of carriers with energy does not change as the relative spin populations vary (keeping the total density constant). However, at lower temperatures or higher carrier densities the required carrier statistics will have a higher degeneracy and there will be a dependence on the relative spin populations. The screened exciton Hamiltonian [Eq. (13)] can be solved variationally[21] or numerically[22] for the $1s$ state. From the change in the wave function ψ_{1s} at $r=0$ in the limit of small screening wave number $a_0\kappa \ll 1$, the relative change in oscillator strength can be determined as $\delta f_{1s}/f_{1s} \simeq -a_0\kappa/2$. Using the above Boltzmann approximation for the screening wave number gives the relative change in exciton oscillator strength due to screening as

$$\frac{\delta f_{1s}}{f_{1s}} = -\pi\frac{E_R^{2D}}{k_bT}a_0^2 n_{\text{total}}^{2D}. \tag{15}$$

This expression for the relative change in oscillator strength in the Boltzmann limit is identical to the exchange term (short-range screening) of Schmitt-Rink *et al.*[2]

The phase-space filling contribution to the change in exciton oscillator strength results from the fact that the exciton is formed out of the plasma plane wave states. If these plane wave states are occupied by free carriers then they are unable to contribute to the exciton states. Therefore for finite carrier densities, the following substitution must be made in the determination of the exciton oscillator strength:[2]

$$\psi_{1s}(r=0) \rightarrow \sum_{\mathbf{k}}(1 - f_{e,\mathbf{k}} - f_{h,\mathbf{k}})\,\psi_{1s}(\mathbf{k}), \tag{16}$$

where $\psi_{1s}(\mathbf{k})$ is the Fourier transform of the unperturbed exciton $1s$ wave function [Eq. (12)],

$$\psi_{1s}(\mathbf{k}) = \frac{\sqrt{2\pi}a_0}{[1+(a_0k/2)^2]^{3/2}}. \tag{17}$$

Since phase-space filling is a consequence of the Pauli exclusion principle, it will only contribute where the exciton and plasma have the same spin states. Using the Boltzmann form for the carrier statistics results in the following expression for the relative change in oscillator strength:

$$\left.\frac{\delta f_{1s}}{f_{1s}}\right|_\sigma = -\pi\sum_{e,h} a_0^2 n_{i,\sigma} F\left(\frac{\mu}{m_i}\frac{E_R^{2D}}{k_bT}\right), \tag{18}$$

where σ refers to the spin state and

$$F(x) = x^{3/2}e^x\Gamma(-1/2, x). \tag{19}$$

It is clear from Eq. (18) that the small signal relative change in the exciton oscillator strength is directly proportional to the plasma density in the same spin state. For the same total carrier density but in the cases of being completely in the opposite spin state (OCP), being equally distributed between the two spin states (OLP), and being completely in the same spin state (SCP), a ratio of the phase-space filling signal of 0:1:2 is expected. In contrast the screening contribution is independent of the relative ratio of spin state occupancy, just depending on the total excited plasma density. For GaAs wells at room temperature, the relevant parameters are estimated as k_bT=25 meV, E_R^{2D}=9 meV (taking the observed binding energy rather than four times the three-dimensional value in a similar manner to Ref. 2), m_e=0.067m_0, m_h=0.34m_0. The screening contribution to the relative change in oscillator strength gives $\delta f/f = -0.36\pi a_0^2 n_{\text{total}}$. In the case of equal populations in each spin state (OLP), summing the electron and hole contributions to phase-space filling gives a relative change in oscillator strength of $\delta f/f = -0.17\pi a_0^2 n_{\text{total}}$. That is, the predicted change in the exciton oscillator strength for GaAs quantum wells at room temperature from screening is roughly double that of phase-space filling for linearly polarized light (i.e., equipopulated spin states). For the three experimental configurations discussed here the predicted oscillator strength changes are $-0.36\pi a_0^2 n_{\text{total}}$, $-0.53\pi a_0^2 n_{\text{total}}$, and $-0.70\pi a_0^2 n_{\text{total}}$ for the OCP, OLP, and SCP cases, respectively. These values can be compared with the peak absorption cross section both for experiment [Fig. 3(a)] and for the numerical approach [Fig. 7(a)] to confirm that Coulombic effects

(spin-independent signal) and phase-space filling (spin-dependent signal) are of similar magnitudes in GaAs quantum wells at room temperature.

IV. DISCUSSION

For GaAs quantum wells under moderate optical excitation at room temperature, the circular dichroism (spin-dependent portion) of the exciton saturation signal is now seen to solely arise from phase-space filling whereas the spin-independent portion derives from the Coulombic effects of exciton screening and broadening. Hence, in the case of opposite circularly polarized beams, initially only Coulombic effects (reduction of the oscillator strength through screening and line-shape broadening) contribute to the exciton saturation. For the other two configurations, the effects of phase-space filling are also perceived, with the effect being increased in the case of the same circularly polarized beams in comparison to the case of orthogonally polarized beams.

It is anticipated that the different contributions to exciton saturation should have different spectral signatures. It has been shown that the effects of phase-space filling and exciton screening are to reduce the oscillator strength and hence reduce the optical absorption over the whole exciton line shape. The effect of line-shape broadening, on the other hand, causes a reduction in optical absorption near line center but an increase in absorption in the wings of the exciton, in such a manner that the area under the exciton line shape remains constant. Thus, line-shape broadening is the only mechanism which can give rise to an increase in absorption in the present configuration due to a photogenerated plasma and its effect will be restricted to the wings of the exciton resonance. It is then clear from Fig. 2 that in the case of the opposite circularly polarized beams (where only the effects of exciton screening and broadening contribute to the exciton saturation), the effects of broadening must be present as there is an increase in absorption in the wings. It is not clear from the estimated absorption cross section whether a reduction of oscillator strength due to screening can be inferred from the present experimental data. Ideally a two-wavelength excite-probe setup could be employed to investigate this further (as the excited carrier density will be independent of the probe wavelength).

It has been shown that the circular dichroism in the heavy-hole exciton saturation arises solely from phase-space filling. The measured dichroism [Fig. 3(b)] has a line shape which reflects the original exciton line shape, i.e., the major effect of phase-space filling is a reduction in oscillator strength. It is also interesting to note that the linear/circular dichroism of the exciton saturation [e.g., $\sigma_\alpha(\mathrm{OLP}) - \sigma_\alpha(\mathrm{OCP})$] is one-half of the circular dichroism in accordance with the predictions of Eq. (18).

The different spectral signatures are also observed in the varying time delay data sets. At the peak of the exciton resonance [Fig. 4(a)], both the contributions to exciton screening and broadening give an absorption decrease so both the spin-dependent (phase-space filling) and spin-independent portions of the signal give a decrease in absorption. It is also important to note that the relative magnitudes of the contributions from phase-space filling and Coulombic effects (exciton screening and broadening) are comparable, in broad agreement with our theoretical predictions. In the wings of the exciton resonance, however, the contributions to the absorption change from exciton screening and broadening have opposite signs. In the particular case examined in Fig. 4(b), the effect of line-shape broadening has the greater magnitude and hence the spin-independent portion of the signal gives an absorption increase. The spin-dependent (phase-space filling) contribution, however, still corresponds to an absorption decrease, giving rise to the observed behavior where there can be some cancellation from the two effects. An example of this is the SCP case on the long wavelength side of the exciton resonance where at zero delay the observed change in the absorption is negligible [Fig. 4(b)].

V. CONCLUSIONS

In conclusion, we have made room temperature, time-resolved measurements of the changes in transmission produced by excitonic saturation at various wavelengths in the vicinity of the heavy-hole exciton resonance. By varying the polarization of the excitation pulse (with respect to the probe pulse), we have been able to alter the occupation of phase-space while leaving the carrier concentration constant.

A theoretical analysis indicates that for small absorption changes and for the applicability of Boltzmann statistics, the circular dichroism of the exciton saturation can be attributed solely to phase-space filling (i.e., a consequence of Pauli exclusion). In the same limit, when excite and probe pulses are circularly polarized in the opposite sense, the observed exciton saturation can be attributed solely to Coulombic effects. Thus we have demonstrated both experimentally and theoretically that the relative contributions to the exciton saturation in GaAs quantum wells at room temperature from phase-space filling and Coulombic effects are of a similar magnitude. This refutes the popular misconception that Coulombic effects are unimportant for GaAs quantum wells at room temperature.

The absorption changes both at the peak of the heavy-hole exciton resonance and on the long wavelength side of the resonance were measured. The observation of an absorption decrease at the peak but an absorption increase on the long wavelength side of the resonance is indicative of a density-dependent broadening. From the measured absorption cross section [Fig. 3(a)], it is clear that this additional Coulombic process is very significant. In the numerical approach the effect of a density-dependent broadening is included, albeit empirically. It is demonstrated that the inclusion of density-dependent broadening can provide an increase in absorption that opposes the absorption decrease from phase-space filling on the long wavelength side of the resonance [compare Figs. 4(b) and 8(b)].

ACKNOWLEDGMENTS

This research was supported in part by the Defense Advanced Research Projects Agency and the Army Research Office. M. J. Snelling gratefully acknowledges support from the Science and Engineering Research Council, D. C. Hutchings from the Royal Society of Edinburgh/Scottish Office Education Department, and I. Galbraith from the Royal Society.

---

* Present address: Clarendon Laboratory, Oxford University, Oxford OX1 3PU, U.K.

† Also with the Center for Research in Electro-Optics and Lasers, University of Central Florida, Orlando, FL 32826.

[1] D. A. B. Miller, Opt. Quantum Electron. **22**, S61 (1990).

[2] S. Schmitt-Rink, D. S. Chemla, and D. A. B. Miller, Phys. Rev. B **32**, 6601 (1985).

[3] W. H. Knox, C. Hirlimann, D. A. B. Miller, J. Shah, D. S. Chemla, and C. V. Shank, Phys. Rev. Lett. **56**, 1191 (1986).

[4] A. Miller, R. J. Manning, P. K. Milsom, D. C. Hutchings, D. W. Crust, and K. Woodbridge, J. Opt. Soc. Am. B **6**, 567 (1989).

[5] J. B. Stark, W. H. Knox, and D. S. Chemla, Phys. Rev. Lett. **68**, 3080 (1992).

[6] S. Bar-Ad and I. Bar-Joseph, Phys. Rev. Lett. **68**, 349 (1992).

[7] V. Srinivas, Y. J. Chen, and C. E. C. Wood, Phys. Rev. B **47**, 10 907 (1993).

[8] M. I. D'Yakonov and V. I. Perel', Zh. Eksp. Teor. Fiz. **60**, 1954 (1971) [Sov. Phys. JETP **33**, 1053 (1971)].

[9] A. G. Aronov, G. E. Pikus, and A. N. Titkov, Zh. Eksp Teor. Fiz. **84**, 1170 (1983) [Sov. Phys. JETP **57**, 680 (1983)].

[10] G. L. Bir, A. G. Aronov, and G. E. Pikus, Zh. Eksp. Teor. Fiz. **69**, 1382 (1975) [Sov. Phys. JETP **42**, 705 (1975)].

[11] G. Fishman and G. Lampel, Phys. Rev. B **16**, 820 (1977).

[12] J. Wagner, H. Schneider, and D. Richards, Phys. Rev. B **47**, 4786 (1993).

[13] A. Tackeuchi, S. Muto, T. Inata, and T. Fujii, Appl. Phys. Lett. **56**, 2213 (1990).

[14] P. Roussignol, P. Rolland, R. Ferreira, C. Delande, G. Bastard, A. Vinattieri, L. Carraresi, M. Colocci, and B. Etienne, Surf. Sci. **267**, 360 (1992).

[15] H. Haug and S. W. Koch, *Quantum Theory of the Optical and Electronic Properties of Semiconductors* (World Scientific, London, 1993).

[16] M. Lindberg and S. W. Koch, Phys. Rev. B **38**, 3342 (1988).

[17] R. Binder, D. Scott, A. E. Paul, M. Lindberg, K. Henneberger, and S. W. Koch, Phys. Rev. B **45**, 1107 (1992).

[18] H. Haug and S. Schmitt-Rink, Prog. Quantum Electron. **9**, 3 (1984).

[19] R. J. Elliot, Phys. Rev. **108**, 1384 (1957).

[20] F. Stern and W. E. Howard, Phys. Rev. **163**, 816 (1967).

[21] J. Lee, H. N. Spector, and P. Melman, J. Appl. Phys. **58**, 1893 (1985).

[22] D. C. Hutchings, Ph.D. dissertation, Heriot-Watt University, Edinburgh, 1988.